Transactions of the Materials Research Society of Japan 31[3] 573-576 (2006)

Control of J-aggregates in the Merocyanine-containing LB Films by Heat Treatments

Syuji Mouri, Junpei Miyata, Shin-ichi Morita*, Yasuhiro F. Miura and Michio Sugi
Graduate School of Engineering, Toin Univ. of Yokohama, 1614 Kurogane-cho, Aoba-ku,Yokohama225-8502, Japan
Fax: 81-45-972-5972, e-mail: sugi@cc.toin.ac.jp
* Present address: Department of Chemistry, The University of Georgia, Athens, GA 30602-2556, U.S.A.

The deconvolution of UV-visible spectra has been carried out for LB films of a merocyanine dye – arachidic acid mixed system in the as-deposited state with a prominent J-band peak, after HT at 90°C without the J-peak, and after heat treatment (HT) at 70°C with a fully developed peak of reorganized J-band. Each spectrum is found to involve three components, Band I, Band II and Band III centered around 510 – 515 nm, 545 – 555 nm and 590 – 600 nm. The dichroic ratios greater than unity for all of the three bands found for the as-deposited films indicate the existence of linkage among the clusters of different aggregation states.
Key words: Langmuir-Blodgett films, Merocyanine chromophores, Control of J-aggregates, Heat treatments

1. INTRODUCTION

The surface-active merocyanine dye MS shown in Fig. 1 (a) is a well-known functional film-forming molecule employed for the trial manufacture of prototypes of photoelectric and memory devices [1-3]. MS forms stable monolayers on an aqueous subphase containing Cd^{2+} ions when it is mixed with arachidic acid (C_{20} in Fig. 1 (b)). They are easily deposited onto substrates to form Y-type LB films using the vertical dipping technique [4-6]. The films are phase-separated into MS-rich and C_{20}-rich domains [7], and blue in color accompanied by a prominent red-shifted band centered around 590 nm, which is identified as a J-band originates from specific aggregation states referred to as J-aggregates [4-7].

The MS aggregation state is found to be modified by various secondary treatments, resulting in drastic changes in the associated properties [8-10]. Heat treatments (HT) as well as acid treatments (AT) dissociate the J-aggregates with the film color changing from blue to red, and basic treatments (BT) restore the aggregates with the color returning to blue [8-10].

As reported in previous papers, the J-band disappears in the spectrum for the LB films with ten or more monolayers when HT at 90°C for 30 min is applied [6, 16]. The film looks now red with a broad spectrum centered around 530 nm, which was often explained to reflect the increased fraction of MS monomers.

Recently, it has been found that narrowing of the red-shifted J-band is thermally induced in the MS-C_{20} mixed Langmuir-Blodgett (LB) films by the "mild" HT at temperatures ranging from 60°C to 70°C [11, 12]. After the mild HT, the original J-band with a prominent in-plane anisotropy becomes sharper in spectral shape with its peak further red-shifted by a few nanometers, and the in-plane anisotropy is drastically decreased at the same time [11, 12]. The observed change is suggested to be due to a total reorganization of the chromophore arrangements rather than an additional growth of the original J-clusters [11, 12]. The reorganization seems to be closely related with the microbrownian motion of alkyl chains which is plausibly assumed to be partially activated even at room temperature [11, 12].

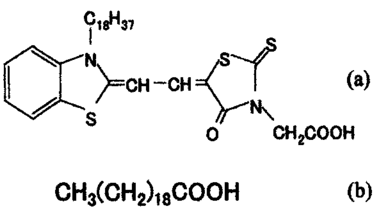

$CH_3(CH_2)_{18}COOH$ (b)

Fig. 1 Chemical formulas of the merocyanine MS (a) and arachidic acid C_{20} (b).

The mild HT is characterized as a purely physical process with a lower risk of degradations, and therefore expected to present another possibility of modifying the properties of LB films. For establishing the mild HT as a means of controlling the aggregation state, it is necessary to know how many bands are involved in each absorption spectrum, and which kind of aggregation state is responsible for each band.

The UV-visible spectra of the MS-containing LB films have been explained as a three-component system involving, e.g., oligomeric (or H-aggregate), monomeric and J-aggregate bands [13, 14]. In this respect, K. Ikagami has recently proposed a novel concept of D-aggregate accompanied by a doublet band, to which he has ascribed the two peaks located at 515nm and 555nm observed in the MS monolayers at the air-water interface, showing that the observed behavior of the spectra is well explained as a two- component system with a doublet D- and a singlet J-bands [15].

We have recently examined the spectra of the MS-C_{20} LB films before and after HT by differentiating them with respect to the wavelength. Three structures have been clearly recognized in each differential spectrum. The results of deconvolution are reported in the present paper.

2. EXPERIMENTAL

Surface-active merocyanine MS and arachidic acid C_{20} (Fig. 1 (a) and (b), respectively) were purchased from Hayashibara Biochemical Laboratories Inc. Kankoh-Shikiso and Fluka AG, respectively, and used without further purification. MS and C_{20} were dissolved in chloroform with a molar ratio of [MS] : $[C_{20}]$=1 : 2. The preparation conditions of LB samples were the same as described in previous papers [11, 12]. The substrates, each 1/4 of an ordinary slide glass, were soaked in an ethanol solution of *pro analysi* grade KOH for 4 – 6 hours, rinsed with pure water, precoated with five monolayers of Cd salt of pure C_{20} to make their surfaces hydrophobic immediately after rinsing, and then ten monolayers of the MS-C_{20} mixture were deposited. The films were of Y-type with a deposition ratio of approximately unity. For the heat treatment, each LB sample was sealed in an aluminum tube with a screw top at one end [11, 12]. The tube was then immersed in a water bath kept at a constant temperature. After a planned heating time, it was pulled out of the bath and cooled down to room temperature. UV-visible spectra $A_{\parallel}$ and $A_{\perp}$ of the LB films were measured at room temperature using a Shimadzu UV-2100 spectrometer, where $A_{\parallel}$ and $A_{\perp}$ refer to absorbances taken using linearly polarized light incidents with the electric vector parallel and perpendicular to the dipping direction in the deposition process, respectively [11, 12].

3. PROCEDURE OF DECONVOLUTION

If a spectrum involves only one simple band characterized as Gaussian or Lorentzian, its differential $dA/d\lambda$ exhibits a peak followed by a valley, where the maximum of A corresponds to $dA/d\lambda$=0 appearing between the summit and the bottom. When two or more bands are involved in a spectrum, each band can be recognized as a shallow valley if the overlap of the neighboring bands is sufficiently small.

Figure 2 exemplifies a differential spectrum, where $dA_{\parallel}/d\lambda$ for the as-deposited case is plotted against the wavelength λ. The curve referred to is an average of $A_{\parallel}$ from 109 LB films to enhance the S/N ratio. We actually recognize three structures, Valleys I, II and III. For each valley, the onset of dip towards the bottom is pointed by a hollow arrow. Here, Valley III corresponds to the J-band (its onset point of dip is out of the plotting area). Similar three-valley structures were also recognized for both HT at 60°C – 70°C and HT at 90°C.

Based on these results, the spectrum for each case is deconvoluted into three bands, Bands I, II and III (J-band), employing the following procedure which consists of four steps.

(1) For Bands I and II, we assume the Gaussian distributions of the form,

$$A(\nu) = \frac{A_0}{\sqrt{2\pi}\sigma}\exp\left\{-\frac{(\nu-\nu_0)^2}{2\sigma^2}\right\}, \tag{1}$$

with the magnitude given by,

$$A_0 \equiv \int_{-\infty}^{+\infty} A(\nu)d\nu, \tag{2}$$

where ν=1/λ is the wavenumber, suffices 0 refer to the band peak, σ denotes the standard deviation, and $\int A(\nu)d\nu$ is a measure of oscillator strength f.

(2) For Band I, the optimum λ_0 is searched for every integer multiple of 5 within the range of Valley I as

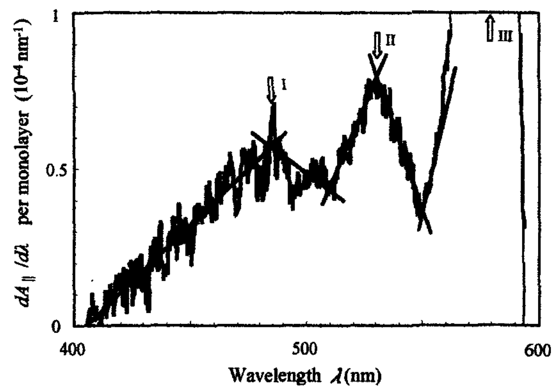

Fig. 2 Differential absorbance $dA_{\parallel}/d\lambda$ for the as-deposited LB films plotted against the wavelength λ. Three structures, Valleys I, II and III, are recognized. For each valley, the onset of dip towards the bottom is pointed by a hollow arrow.

giving the best fit to the spectrum in the range of 400 nm – 470 nm by adjusting the values of A_0 and σ. Thus estimated A^{I} for Band I is subtracted from the original A.

(3) For Band II, the optimum λ_0, A_0 and σ are estimated in a similar manner as in Step (2), where the spectrum to fit is now $A - A^{\mathrm{I}}$ in the spectral range of 460 nm – 520 nm. Thus obtained A^{II} is subtracted from $A - A^{\mathrm{I}}$.

(4) The remainder $A - A^{\mathrm{I}} - A^{\mathrm{II}}$ is assumed to correspond to Band III representing the J-band, i.e., $A^{\mathrm{III}} = A - A^{\mathrm{I}} - A^{\mathrm{II}}$, if it is larger than –(noise level, ~ -10^{-4}, typically) everywhere in the entire range of λ. When this criterion is not satisfied, one should then go back to Step (3) to make a compromise by reducing the upper limit of the range for the fitting of A^{II}.

4. RESULTS AND DISCUSSION

The above described procedure has been applied to three different cases: the spectra in the as-deposited state (Case -1), after HT at 90°C with the prominent J-band peak almost completely vanished (Case-2), and after mild HT at 70°C with the reorganized J-band fully developed (Case-3).

The deconvoluted spectra are shown together with the measured ones in Figs. 3, 4 and 5 for Case-1, Case-2 and Case-3, respectively. Table I summarizes the values of parameters estimated. For each case, Step (2) for Band I is found to be effective for reproducing the measured spectrum for wavelengths λ < 460 nm, indicating the plausibility of Gaussian approximation. Step (3) for Band II is also satisfactory except for Case-2, where the wavelength upper limit is reduced down to 510 nm to make the compromise.

4. 1 Case-1 – as-deposited spectra

The measured spectra for Case-1, $A_{\parallel}$ and $A_{\perp}$, in Figs. 3(a) and (b) coincide with the corresponding as-deposited spectra reported previously [4-6]: each with a prominent J- band with an in-plane anisotropy of $A_{\parallel}/A_{\perp}$>1.

Band I and Band II share the same set of λ_0- and σ-values for both polarization directions. The values, λ_0 =500 nm for Band I and 545 nm for Band II, respectively, may be assigned either to the oligomers and monomers or to the doublet D-band.

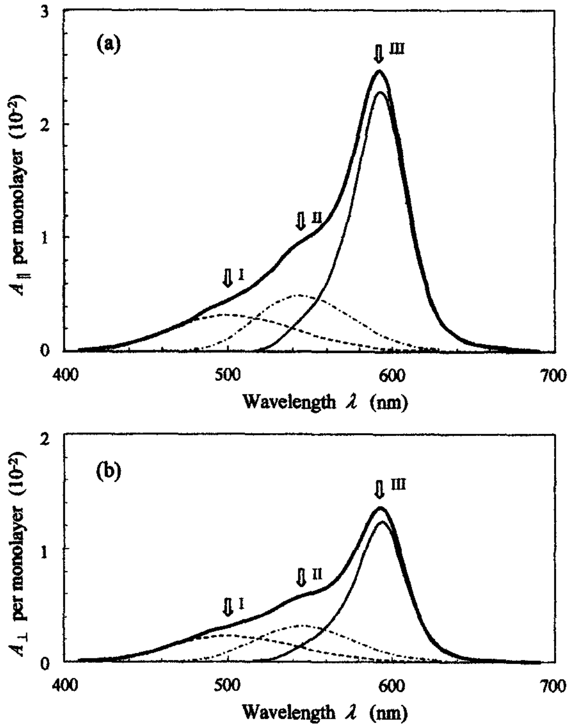

Fig. 3 Case-1. The measured and deconvoluted spectra in the as-deposited state for the (a) parallel and (b) perpendicular incidents. The thick solid, thin dashed, thin chain, and thin solid lines refer to A, A^{I}, A^{II} and A^{III}, respectively. The peak positions of Bands I, II and III are pointed by the hollow arrows.

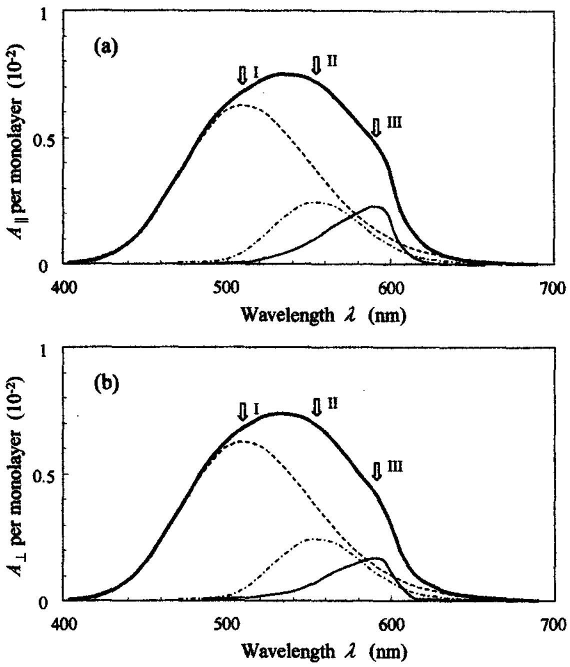

Fig. 4 Case-2. The measured and deconvoluted spectra after HT at 90°C for the (a) parallel and (b) perpendicular incidents. The thick solid, thin dashed, thin chain, and thin solid lines refer to A, A^{I}, A^{II} and A^{III}, respectively. The peak positions of Bands I, II and III are pointed by the hollow arrows.

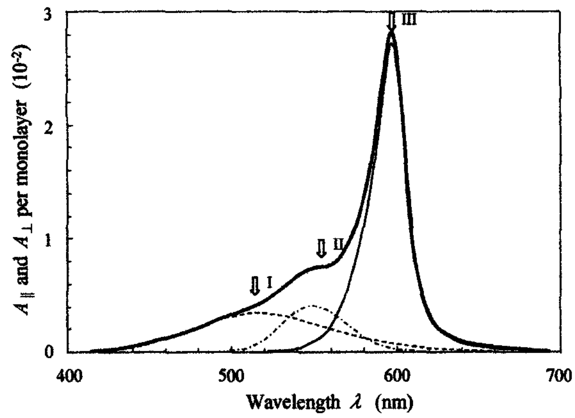

Fig. 5 Case-3. The measured and deconvoluted spectra after HT at 70°C. The thick solid, thin dashed, thin chain, and thin solid lines refer to A, A^{I}, A^{II} and A^{III}, respectively. The peak positions of Bands I, II and III are pointed by the hollow arrows.

Table I Values of parameters for each case.

Case-1	$A_{\parallel}$	$A^{\mathrm{I}}_{\parallel}$	$A^{\mathrm{II}}_{\parallel}$	$A^{\mathrm{III}}_{\parallel}$
λ_0 (nm)	593.6	500	545	594.4
ν_0 (cm^{-1})	16846	20000	18348	16823
σ (cm^{-1})	---	1537	982	---
$\int A(\nu)d\nu$ (cm^{-1})	55.79	12.43*	12.31*	31.05
f/f_{total} (%)	100.0	22.3	22.1	55.6
	$A_{\perp}$	$A^{\mathrm{I}}_{\perp}$	$A^{\mathrm{II}}_{\perp}$	$A^{\mathrm{III}}_{\perp}$
λ_0 (nm)	594.0	500	545	594.8
ν_0 (cm^{-1})	16835	20000	18348	16812
σ (cm^{-1})	---	1537	982	---
$\int A(\nu)d\nu$ (cm^{-1})	32.45	9.07*	7.64*	15.73
f/f_{total} (%)	100.0	28.0	23.5	48.5
Case-2	$A_{\parallel}$	$A^{\mathrm{I}}_{\parallel}$	$A^{\mathrm{II}}_{\parallel}$	$A^{\mathrm{III}}_{\parallel}$
λ_0 (nm)	533.8	510	555	590.0
ν_0 (cm^{-1})	18734	19608	18018	16949
σ (cm^{-1})	---	1537	884	---
$\int A(\nu)d\nu$ (cm^{-1})	32.82	24.08*	5.40*	3.34
f/f_{total} (%)	100.0	73.4	16.4	10.2
	$A_{\perp}$	$A^{\mathrm{I}}_{\perp}$	$A^{\mathrm{II}}_{\perp}$	$A^{\mathrm{III}}_{\perp}$
λ_0 (nm)	533.4	510	555	590.0
ν_0 (cm^{-1})	18748	19608	18018	16949
σ (cm^{-1})	---	1537	884	---
$\int A(\nu)d\nu$ (cm^{-1})	31.88	24.08*	5.40*	2.40
f/f_{total} (%)	100.0	75.5	17.0	7.5
Case-3	A**	A^{I}	A^{II}	A^{III}
λ_0 (nm)	598.0	515	555	598.2
ν_0 (cm^{-1})	16722	19417	18018	16717
σ (cm^{-1})	---	1537	643	---
$\int A(\nu)d\nu$ (cm^{-1})	42.69	13.06*	6.45*	23.18
f/f_{total} (%)	100.0	30.6	15.1	54.3

*) $\int A(\nu)d\nu = A_0$ for A^{I} and A^{II}, see Eq. (2).
**) $A = A_{\parallel} = A_{\perp}$.

Band III given as the remainder in the present procedure can be identified with the J-band. Thus obtained $A^{III}_{\parallel}$ and $A^{III}_{\perp}$ spectra resemble to each other. Indeed, the values of dichroic ratio estimated in two different ways approximately coincide with each other, $A^{III}_{\parallel\,max}/A^{III}_{\perp\,max}$=1.85 and $\int A^{III}_{\parallel}(\nu)d\nu/\int A^{III}_{\perp}(\nu)d\nu$=1.97.

Band I and Band II also exhibit dichroic ratios greater than unity: $A^{I}_{0\,\parallel}/A^{I}_{0\,\perp}$=1.37, $A^{II}_{0\,\parallel}/A^{II}_{0\,\perp}$=1.61. This coincidence suggests that there exists a certain superstructure linking together the clusters in different aggregation states when they are subjected to the flow orientation effect during the transfer from the water surface onto the substrate [16].

4. 2 Case-2 – after HT at 90°C

The spectra for both polarization directions reproduce those reported previously [8, 10]. They are shown in Figs. 4(a) and (b), respectively. The prominent J-band peak is no more to be seen, and Band I and Band II are now isotropic with $A^{I}_{\parallel}=A^{I}_{\perp}$ and $A^{II}_{\parallel}=A^{II}_{\perp}$, each given by the same values of parameters as given in Table I. The linkage among the clusters is therefore lost during the chromophore rearrangement induced by HT. The peak positions, λ^{I}_{0}=510 nm and λ^{II}_{0}=555 nm, are by 10 nm red-shifted from the corresponding values for Case-1. This red-shift may be due to a cancellation of blue-shift in the as-deposited state caused by the HT-induced breakage of links. The values of total magnitude $\int A(\nu)d\nu$ of Band I and Band II are appreciably increased and decreased, respectively, compared to those for Case-1 for both polarization directions.

Although the J-band (Band III) is still recognized for both polarization directions, the oscillator strengths are drastically reduced down to 10.8% and 15.3% of those of Case-1 for both parallel and perpendicular directions, respectively, as calculated from the data in Table I. The coincidence of the two different values of dichroic ratio, $A^{III}_{\parallel\,max}/A^{III}_{\perp\,max}$=1.34 and $\int A^{III}_{\parallel}(\nu)d\nu/\int A^{III}_{\perp}(\nu)d\nu$=1.39, results from the similarity in shape of both spectra, suggesting the plausibility of the present deconvolution.

4. 3 Case-3 – after HT at 70°C

As shown in Fig. 5, the in-plane anisotropy is no more to be seen. The measured spectra for the parallel and perpendicular incidents are identical with each other ($A= A_{\parallel}= A_{\perp}$) [11, 12], suggesting the complete breakage of links among the clusters.

The peak position, λ^{I}_{0}=515 nm, for Band I is by 5 nm more red-shifted, while λ^{II}_{0}=555 nm for Band II is identical with that for Case-2 as given in Table I. A remarkable feature is the decreased contribution of Band II to the total oscillator strength f/f_{total} down to 6.45% with an appreciably smaller value of deviation σ.

The reorganized J-band (Band III) is sharper in spectral shape than the original J-band component of Case I, and it is further red-shifted by a few nanometers as reported previously [11, 12].

The total magnitude $\int A(\nu)d\nu$=42.69 cm^{-1} and the fraction of oscillator strength f^{III}/f_{total}=54.3% for Case-3 satisfactorily coincide with the corresponding averages for Case-1, $(\int A_{\parallel}(\nu)d\nu + \int A_{\perp}(\nu)d\nu)/2$=44.12 cm^{-1} and $(f^{III}_{\parallel}+f^{III}_{\perp})/(f_{\parallel\,total}+f_{\perp\,total})$=53.0%, respectively. MS chromophores are therefore well conserved during HT.

5. CONCLUDING REMARKS

We have described the results of deconvolution of UV-visible spectra of MS-C_{20} mixed LB films in the as-deposited state with a prominent J-band peak (Case-1), after HT at 90°C without the J-peak (Case-2), and after HT at 70°C with a fully developed peak of reorganized J-band (Case-3). The procedure adopted is of empirical nature starting from three structures observed in the differential spectra. For all the three cases, the spectra are found to involve three bands, Band I, Band II and Band III centered at 510 – 515 nm, 545 – 555 nm and 590 – 600 nm, respectively. Band III is plausibly assigned to the J-aggregates. Bands I and II may be compared to oligomers, monomers, respectively, in the three-component model [13], while the both may be assigned to the D-aggregate according to Ikegami's two-component model [15]. In the present stage, however, nothing decisive can be said as to the origin of these two bands.

As for Case-I, Band I and Band II as well as Band III are found to be associated with dichroic ratios greater than unity, suggesting the existence of linkage among the different kinds of chromophore clusters.

The invariance of oscillator strengths of the original and the reorganized J-bands indicates the possibility of the mild heat treatment as an effective method of modifying the physical properties of LB films with lesser risk of degradation of the film quality in comparison to the acid, the basic and other chemical treatments.

REFERENCES

[1] M. Saito, M. Sugi, T. Fukui and S. Iizima, Thin Solid Films **100**, 117 (1983).

[2] K. Sakai, M. Saito, M. Sugi and S. Iizima, Jpn. J. Appl. Phys. **24**, 865 (1985).

[3] M. Sugi, K. Sakai, M. Saito, Y. Kawabata and S. Iizima, Thin Solid Films **132**, 69 (1985).

[4] M. Sugi and S. Iizima, Thin Solid Films **68**, 199 (1980).

[5] M. Sugi, T. Fukui, S. Iizima and K. Iriyama, Mol. Cryst. Liq. Cryst. **62**, 165 (1980).

[6] M. Sugi, M. Saito, T. Fukui and S. Iizima, Thin Solid Films **88**, L15 (1982).

[7] M. Sugi, M. Saito, T. Fukui and S. Iizima, Thin Solid Films **99**, 17 (1983).

[8] M. Sugi, M. Saito, T. Fukui and S. Iizima, Thin Solid Films **129**, 15 (1985).

[9] T. Fukui, M. Saito, M. Sugi and S. Iizima, Thin Solid Films **109**, 247 (1983).

[10] M. Saito, M. Sugi, K. Ikegami, M. Yoneyama and S. Iizima, Jpn. J. Appl. Phys. **25**, L478 (1986).

[11] J. Miyata, S. Morita, Y. F. Miura and M. Sugi, Jpn. J. Appl. Phys. **44**, 8110 (2005).

[12] J. Miyata, S. Morita, Y. F. Miura and M. Sugi, Colloids and Surfaces. **A** (2006), in press.

[13] Y. Hirano, T. M. Okada, Y. F. Miura, M. Sugi and T .Ishii, J. Appl. Phys. 88, 5194 (2000).

[14] K. Ray and H. Nakahara, Jpn. J. Appl. Phys. **40**, 5095 (2001).

[15] K. Ikegami, J. Chem. Phys. **121**, 2337 (2004).

[16] N. Minari, K. Ikegami, S. Kuroda, K. Saito, M. Saito and M. Sugi, J. Phys. Soc. Jpn. **58**, 222 (1989).

(Received December 10, 2005;Accepted March 7, 2006)